

# TRIBOLOGICAL PROPERTIES OF COMPOCASTED A356 ALUMINIUM ALLOY COMPOSITE REINFORCED WITH Al<sub>2</sub>O<sub>3</sub>, SiC AND GRAPHITE PARTICLES<sup>1</sup>

Aleksandar Venci<sup>2</sup>  
Saioa Arostegui<sup>3</sup>  
Ilija Bobic<sup>4</sup>

## Abstract

Particulate composites with A356 aluminium alloy as a matrix were produced by compocasting process using ceramic particles (Al<sub>2</sub>O<sub>3</sub>, SiC) and graphite particles. The matrix alloy and the composites were thermally processed applying the T6 heat treatment regime. Hardness and tribological properties of heat treated matrix alloy and composites were examined and compared. Tribological tests were carried out on pin-on-disc tribometer under dry sliding conditions. Sliding was linear (reciprocating). Counter body was alumina ball. Maximum velocity was 0.06 m/s, sliding distance was 500 m and normal load was 1 N. Wear resistance of the composites reinforced with SiC particles was higher and coefficient of friction was lower compared to the composite reinforced with Al<sub>2</sub>O<sub>3</sub> particles due to the higher hardness of the SiC particles, and due to the fact that the SiC reinforcements were protruded to the surface and thus protect the matrix alloy from further wear. Addition of graphite particles (1 wt. %) to the composite with SiC particles further reduced the wear rate and the coefficient of friction.

**Keywords:** A356 alloy; Metal matrix composites; Graphite particles; Wear; Friction.

<sup>1</sup> Technical contribution to the First International Brazilian Conference on Tribology – TribobR-2010, November, 24<sup>th</sup>-26<sup>th</sup>, 2010, Rio de Janeiro, RJ, Brazil.

<sup>2</sup> Tribology Laboratory, Mechanical Engineering Faculty, University of Belgrade, Kraljice Marije 16, 11120 Belgrade 35, Serbia, [avenci@mas.bg.ac.rs](mailto:avenci@mas.bg.ac.rs)

<sup>3</sup> CSM Instruments SA, Rue de la Gare 4, CH-2034 Peseux, Switzerland, [saioa.arostegui@csm-instruments.com](mailto:saioa.arostegui@csm-instruments.com)

<sup>4</sup> Institute of Nuclear Science “Vinca”, Mike Petrovića Alasa 12-14, 11001 Belgrade, Serbia, [ilijab@vinca.rs](mailto:ilijab@vinca.rs)

## 1 INTRODUCTION

Aluminium matrix composites have wide range of applications in automotive and other industries regarding respectable advantages compared to the unreinforced materials such are: reduced density (weight); improved stiffness and damping capabilities; thermal/heat management; enhanced electrical performances; respectable improvement of tribological properties etc.<sup>(1)</sup> A356 aluminium alloy is a casting alloy consisting of aluminium, silicon and magnesium. It is distinguished by good mechanical characteristics and high ductility, as well as excellent casting characteristics and high corrosion resistance. This alloy has been used for many years as a matrix for composites with ceramic reinforcing particles and fibres such as SiC, Al<sub>2</sub>O<sub>3</sub> etc.<sup>(2-4)</sup> aiming to improve the alloy wear resistance. However for applications where features such as improved seizure resistance and reduced friction are of importance a hybrid aluminium matrix composites with solid lubricant (mostly graphite) addition have been developed.<sup>(5)</sup>

The properties of aluminium alloy/graphite particulate composites have been analysed by many authors. Liu, Rohatgi and Ray<sup>(6)</sup> studied friction and wear behaviour of 2014 Al-Si alloy matrix composite with high graphite particles content (50 vol. %). They found that the coefficients of friction and wear were significantly lower in the composite, as compared to those in the matrix alloy. The transition to severe wear took place at a higher load and sliding speeds as compared to the matrix alloy, as well. The controlling factor was the graphite film formation between the rubbing surfaces. The same authors in another study<sup>(7)</sup> showed that in low graphite content composites wear rate decreases with increasing of sliding speed as the graphite film thickness and extension increases. In larger graphite volume fractions wear rate is very low and becomes in fact independent of sliding speed due to graphite film stability. For graphite contents higher than 20 vol. % the graphite film grows thicker, resulting in its delaminating without affecting the overall wear resistance of composites. Basavarajappa et al.<sup>(8)</sup> investigated dry sliding wear behaviour of matrix 2219 aluminium alloy and composite with SiC and graphite particles. They found that the addition of SiC and graphite reinforcements increases the wear resistance of the composites comparing to the matrix alloy. They also found that addition of even a relatively small amount of graphite (3 %) to the Al/SiC composite increases the wear resistance of the composites. Yang et al. [9], investigating A356.2 aluminium/graphite particle composites, concluded that for composites with graphite in small content (around 2 wt. %) the formed lubricant film could not effectively decrease the friction coefficient. Increasing of the graphite addition up to 6 wt. % decrease the coefficient of friction and wear rate but greater amount of graphite does not show further significant improvements of the coefficient of friction and even tends to increase the wear rate of composite.

Particulate reinforced composites cost less than fibre reinforced composites, owing to the lower costs of the particles. In addition, the mechanical and physical properties of particle composites are generally isotropic. Cast metal matrix particulate composites represent the lowest cost composites, and these have found the most tribological applications.<sup>(7)</sup>

In this paper the tribological properties under dry sliding conditions of three aluminium matrix composites were analysed and compared between themselves and with the matrix alloy. The composites were produced by compocasting process using ceramic particles (Al<sub>2</sub>O<sub>3</sub>, SiC) and graphite particles as reinforcement.

## 2 MATERIALS AND PROCEDURE

### 2.1 Materials

The matrix material was A356 hypoeutectic Al-Si alloy (EN AlSi7Mg0.3) with the following chemical composition (in wt. %): Al-7.2Si-0.02Cu-0.29Mg-0.01Mn-0.18Fe-0.01Zn-0.02Ni-0.11Ti.

Composites were produced by the compocasting process using mechanical mixing of the matrix, i.e. Al<sub>2</sub>O<sub>3</sub>, SiC and graphite particles as reinforcement were added into the semi solid A356 alloy by infiltration and admixing. The average size of Al<sub>2</sub>O<sub>3</sub> and SiC particles was 35 µm and 39 µm, whereas the amount of particles was 10 wt. %. Graphite particles size was 35 µm and amount of particles was 1 wt. %. Experimental procedure and apparatus used for the compocasting processing are described and discussed elsewhere.<sup>(10,11)</sup>

Four sets of specimens were used for testing, fabricated from:

- composite material with 10 wt. % Al<sub>2</sub>O<sub>3</sub> of 35 µm particles size (referred as 10-35),
- composite material with 10 wt. % SiC of 39 µm particles size (referred as 10-39),
- composite material with 10 wt. % SiC of 39 µm particles size and 1 wt. % graphite of 35 µm particle size (referred as 10-39-1), and
- matrix alloy (referred as A356).

All specimens were subjected to heat treatment with following parameters: solution annealing at 540 °C for 6 hours, water quenching and artificial aging at 160 °C for 6 hours. Microstructure of the tested materials were presented and discussed elsewhere.<sup>(10)</sup>

### 2.2 Hardness Measurement

Hardness measurements were carried out using a CSM micro indentation tester and applying the Instrumented indentation technique.<sup>(12,13)</sup> The scheme and photography of the CSM device is given in Figure 1.

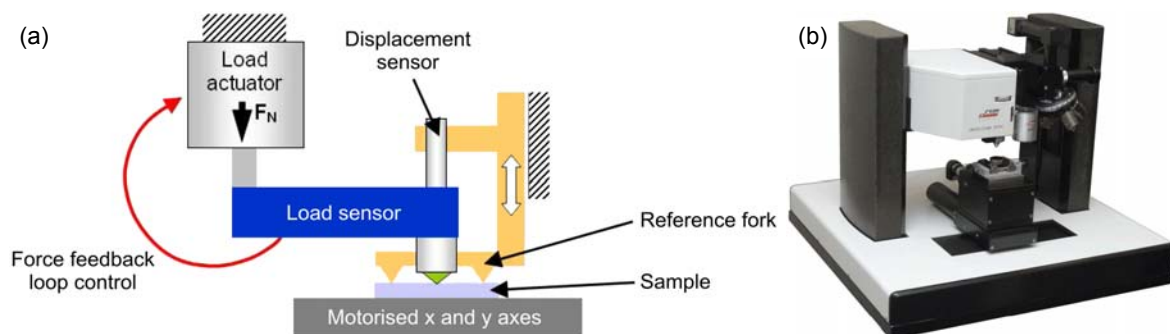


**Figure 1.** CSM micro indentation tester: (a) schematic diagram and (b) photography.

The micro indentation tester uses an already established method where an indenter tip with a known geometry is driven into the specific site of the material to be tested, by applying an increasing normal load. When reaching the pre-set maximum value, the normal load is reduced until partial or complete relaxation occurs. At each stage of the experiment the position of the indenter relative to the sample surface is precisely monitored with a differential capacitive sensor. This procedure was performed repetitively in ambient air, at temperature of 23 °C and humidity of 40 %. The following indentation parameters were used to produce several indents on each

sample (six to twelve depending on the tested material in order to eliminate possible segregation effects): indenter Vickers; contact load 10 mN; loading rate 2 N/min; maximum load 1 N and pause at maximum load 15 s. For reinforcement particles (Al<sub>2</sub>O<sub>3</sub>, SiC), hardness measurements was done with smaller maximum load of 0.15 N.

### 2.3 Tribological Tests Procedure

Tribological tests were carried out on the CSM pin-on-disc tribometer under dry sliding conditions, in ambient air, at temperature of 23 °C and humidity of 40 %. Tribometer test mode was linear (reciprocating) movement. Static body (counter body) was a 6 mm diameter alumina ball. Moving body with cylindrical geometry, having 5 mm diameter and 20 mm length, were made from tested materials and used as test samples instead of disc. Schematic diagram and photography of the tribometer are shown in Figure 2. In order to achieve a higher confidence level in evaluating test results, three to four replicate tests were run for all the tested materials.

Total wear track length on the reciprocating moving test samples was 5 mm. Maximum test samples velocity was 0.06 m/s and the average one was app. 0.038 m/s. Stop condition for all tests was 50000 cycles i.e. after  $1.31 \cdot 10^4$  s, which gave a total sliding distance of 500 m. A constant normal load of 1 N was maintained during all tests.

Before testing, both the test sample and the counter body were degreased and cleaned with isopropyl alcohol. After testing the wear track profiles on the test samples were measured with Taylor Hobson profilometer (Figure 3a). Three wear track profiles (one on each extremity and another one on the centre) were taken on each sample (Figure 3b). There was a difference between the surface area measured at the centre and the extremities, so for the wear volume calculation an average value of the three measurements was used.

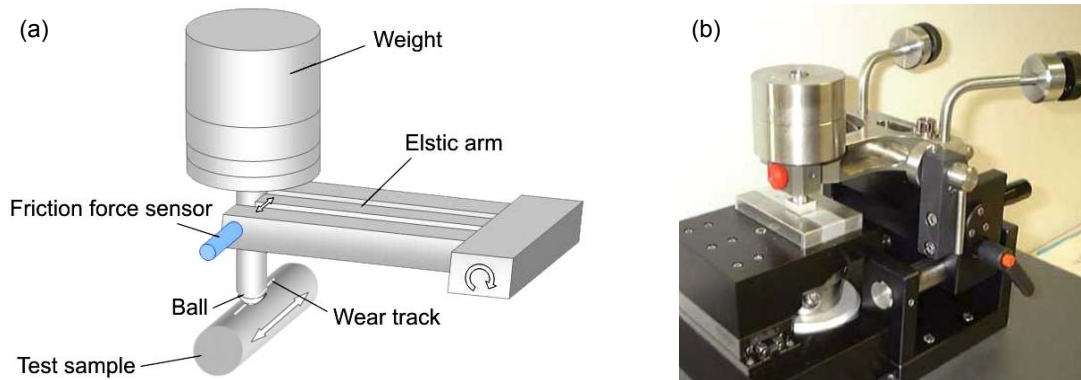


**Figure 2.** CSM pin-on-disc tribometer: (a) schematic diagram and (b) photography.

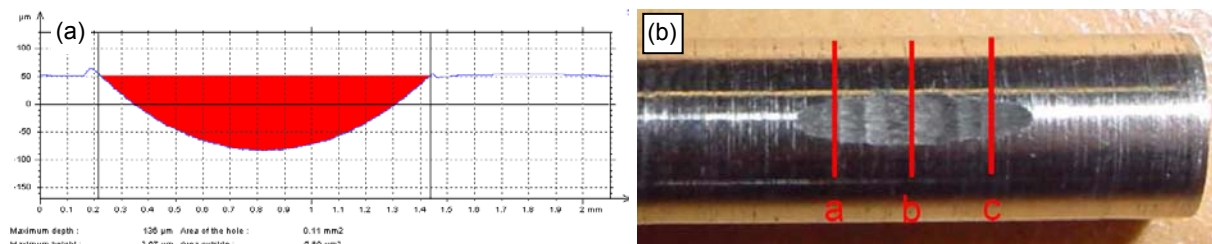


**Figure 3.** Measuring of the wear track profile: (a) profile appearance and measured area surface and (b) positions of the wear track profiles.

The value of friction force was monitored during the test and through data acquisition system stored in the PC, enabling the calculation of friction coefficient. Worn surfaces of counter body and test samples were observed after testing using optical microscopy (OM) and scanning electron microscopy (SEM). Generated wear debris were additionally examined with SEM equipped with energy dispersive spectrometer (EDS).

### 3 RESULTS AND DISCUSSION

#### 3.1 Hardness

The values of hardness for tested materials are shown in Table 1. The coefficient of variation ( $V_r$ ) was calculated as a standard deviation divided by the average value and multiplied with 100 %. As it can be seen the repeatability of the hardness test results for composite materials was very poor (especially for the composite 10-39-1). This is more obvious if we compare test curves for A356 matrix alloy and composite 10-39-1 (Figs. 4a and b, respectively). The hardness of reinforcement particles was also measured in order to verify the value of these particles (Table 1).

**Table 1.** Obtained average values from the hardness testing

Material	Microhardness HV <sub>0.1</sub> *	Coefficient of variation V <sub>r</sub> , %
A356 matrix alloy	151.5	5.7
Composite 10-35	173.5	22.9
Composite 10-39	100.8	14.6
Composite 10-39-1	104.5	30.7
Al <sub>2</sub> O <sub>3</sub> particle	2285.4	13.0
SiC particle	3642.5	8.5

\*HV<sub>0.015</sub> for Al<sub>2</sub>O<sub>3</sub> and SiC particles.

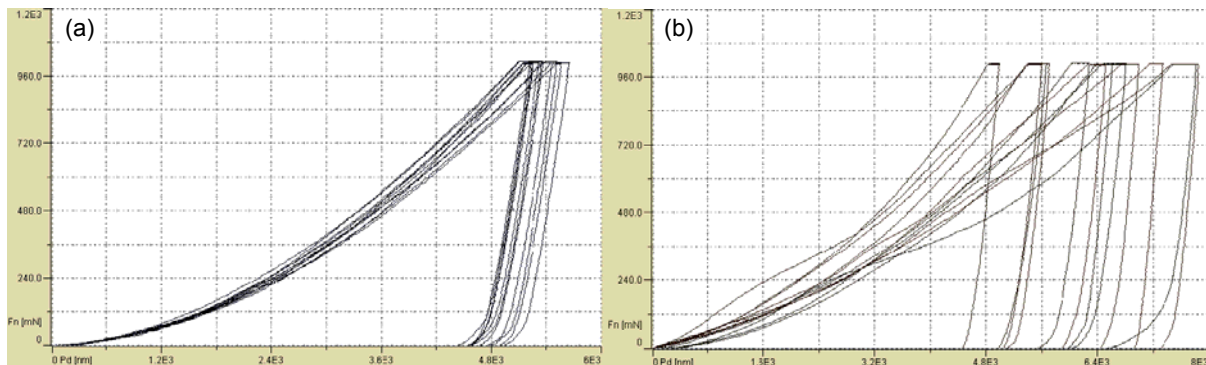


**Figure 4.** Load versus penetration depth curves for: (a) A356 matrix alloy and (b) composite 10-39-1.

The indentations done on a specific reinforcement particle show that the particles are in fact very hard and that the results correspond to values found in literature for this kind of particles (Table 1). Hardness of the composite with Al<sub>2</sub>O<sub>3</sub> particles showed the highest value, while the composites with SiC particles hardness were unexpectedly low. The reason of these results can be several. It is possible that the particles and the matrix are not well “bonded” or that there are some voids and porosity on the composite material. In metal matrix composites, mechanical properties depend on the mechanical properties of the matrix material and the nature of the interface as well as on the amount, size, shape and distribution of the dispersed phase.<sup>(7)</sup> The fact that the composites with SiC particles

had lower values of hardness than the composites with  $Al_2O_3$  particles (and even lower than matrix alloy) induced some further tests of these material.<sup>(10)</sup>

In the case of A356 matrix alloy higher hardness of heat treated samples in comparison to as cast samples are the result of significant structural changes during heat treatment.<sup>(11)</sup> First of all the hardening of the alloy structure (age hardening) takes place and in addition, the inhomogeneous dendritic structure of the matrix transforms to a fine nodular structure. The consequence of this structure is the uniformity of mechanical and tribological properties that are characteristic for homogeneous materials.

### 3.2 Wear Properties

The shape of the wear track was not the same for all tested materials. The width of the wear track was widest at the centre of the sample but the difference of the wear track width measured at the centre and the extremities was different. This difference was biggest for A356 matrix alloy (Figure 5a), than for composites 10-35 and 10-39 (Figure 5b), while for composite 10-39-1 the track width remained more or less constant (Figure 5c).



**Figure 5.** Wear track appearance: (a) A356 matrix alloy, (b) composite 10-35 and (c) composite 10-39-1.

Obtained average values of the wear testing are presented in Figure 6. The results indicate good repeatability of the test, except for the composite 10-39-1. The coefficient of variation ( $V_r$ ) was calculated in the same way as for the hardness test results. The smallest coefficient of variation values was for A356 matrix alloy since it was a most homogeneous material according to the some previous results.<sup>(10)</sup>

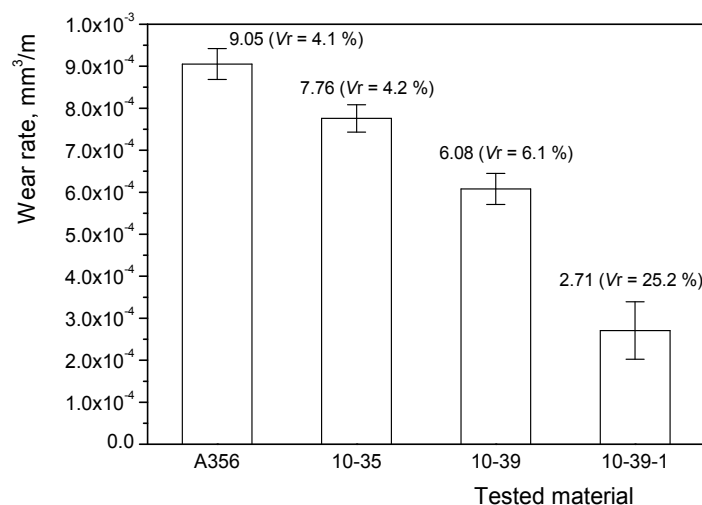


**Figure 6.** Obtained average values from the wear testing.

The composites showed improved wear resistance compared to the A356 matrix alloy which was expected. Higher wear resistance of the composites reinforced with SiC particles in relation to the composite reinforced with Al<sub>2</sub>O<sub>3</sub> particles is in correlation with research conducted by Rohatgi, Liu and Ray.<sup>(7)</sup> This can be explained by the favourable arrangement of SiC reinforcing particles in the composite matrix,<sup>(10)</sup> i.e. the area without particles in the matrix is reduced, which have caused more uniform wear and better protection of the surface. Also the hardness of the SiC particles was higher (Table 1). The results of the wear testing are not completely in correlation with the hardness values of the tested materials. The two composites 10-39 and 10-39-1 showed lower values of wear rates than composite 10-35 since the SiC reinforcement is much harder than the Al<sub>2</sub>O<sub>3</sub> reinforcement despite the fact that they showed relatively low values of hardness.

Lower values of wear rates of the composite 10-39-1 comparing to the composite 10-39 is probably due to the fact that during the sliding protruded SiC particles fracture and lead to the abrasive wear. However, at places where graphite particles are present, the fractured SiC particles easily penetrate into the matrix alloy due to the low hardness, squeezing some of the graphite from the matrix. The graphite particles smear at the interface between the contact bodies and reduce the coefficient of friction. Hence, the heat generated due to friction is also reduced. This is in correlation with the results of Basavarajappa et al.<sup>(8)</sup> who investigated dry sliding wear behaviour of aluminium matrix composite with SiC and graphite particles with similar particles average sizes (25 µm and 45 µm, respectively). They found that addition of even a relatively small amount of graphite (3 %) to the Al/SiC composite increases the wear resistance of the composites.

### 3.3 Coefficient of Friction

Results of the friction testing are presented in Table 2. First it can be noticed that the running-in period was not the same for all tested materials. The longest running-in period was noticed with composite 10-35 (Figure 7a), and the shortest for the composite 10-39-1 (Figure 7b). The shortest value noticed at composite 10-39-1 is expected since this composite contained graphite which acts as a solid lubricant, but the value at matrix alloy is unexpected. The reason for this is probably the plastic deformation of the material and its transfer to the counter body (see Sec. 3.4).

**Table 2.** Obtained average values from the friction testing

Material	A356 matrix alloy	Composite 10-35	Composite 10-39	Composite 10-39-1
Running-in distance, m	200	270	170	130
Steady state period coefficient of friction (after 300 m)	0.67	0.73	0.71	0.65
Coefficient of variation $V_r$ , %	2.8	28.0	8.0	14.8

The shape of the coefficient of friction curve was also different. For the composites 10-35 and 10-39 it was rising from the beginning of the testing until it reached steady state value, probably because the hardness difference of the reinforcements and the matrix was very high. On the other hand for the A356 and composite 10-39-1 coefficient of friction curve rises from the beginning and then goes down to the steady state value, probably due to the plastic flow of the material (A356) and squeezing and smearing of the graphite (composite 10-39-1).

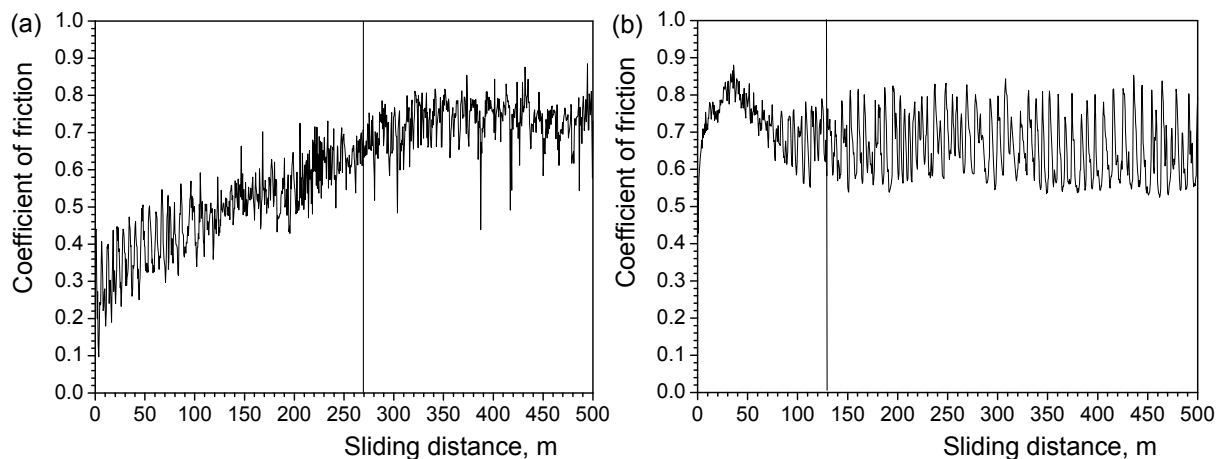


**Figure 7.** The running-in period and the shape of coefficient of friction curve for: (a) composite 10-35 and (b) composite 10-39-1.

Attained values of the coefficient of friction were in expected range for light metals in dry sliding conditions, and all tested materials show very similar values of friction coefficient (Table 2). Values of the coefficient of friction for the composites correspond to the wear rate values of those materials. Generally for all composites values of the coefficient of friction are higher comparing to the matrix alloy. An exception is composite 10-39-1 probably due to the fact that small amount of graphite (1 wt. %) was present in this composite. Rohatgi, Liu and Ray<sup>(7)</sup> conducted a study in which they concluded that when the volume fraction of graphite in the composite is greater than 20 vol. %, the coefficient of friction is close to 0.2 regardless of the matrix. In other cases it is much higher. Having this in mind and since the coefficient of variation of the coefficient of friction for composite 10-39-1 was also relatively high and since the presence of graphite was small this should be considered with caution and only noticed as a possible trend of behaviour.

It is commonly known that the size of the particles for composites that contain soft particles affects the wear rates and coefficients of friction of composites under sliding wear conditions i.e. the larger the particles, the lower the wear rate and coefficient of friction.<sup>(7)</sup> In composite 10-39-1 original graphite particles average size was 35  $\mu\text{m}$ , but they did not keep their average size during compocasting. In the research conducted by Yang et al.<sup>(9)</sup> it was concluded that for composites with graphite particles (with average size of 15  $\mu\text{m}$ ) in small content (around 2 wt. %) the formed lubricant film could not effectively decrease the friction coefficient, while the increasing of the graphite particle addition over 6 wt. % does not show significant improvements of the coefficient of friction and even tends to increase the wear rate of composite. It is also well known that the effect of sliding velocity on wear rate is more complex for composites that contain soft particles. Rohatgi, Liu and Ray<sup>(7)</sup> in their article specify an example that the wear rate for an aluminium alloy composite containing 5 % graphite decreases with increasing sliding speed (0.5 to 5 m/s), which is applicable to this study since the sliding speed in our case was relatively small (app. 0.038 m/s). It is obvious that for each case there exists a range of optimal value of graphite particle content to produce material with good tribological properties.



### 3.4 Worn Surfaces Analysis

After the visual inspection, analysis of the test samples worn surfaces was performed at the end of tests with SEM (Figures 8 and 9). Worn surfaces of A356 matrix alloy (Figures 8a and b) and composite 10-35 (Figures 8c and d) showed similar appearance. Significant smearing as a result of material plastic flow could be noticed on both materials. This smearing was less pronounced for composite 10-35 which corresponds to the wear rate values of these two materials. Dominant type of wear was adhesive wear with adhesive plates of deformed material and presence of wear debris caused by fracture, accumulated into the adhesive wear pits (denoted by arrows in Figures 8b and d). Presence of the reinforcement ( $\text{Al}_2\text{O}_3$ ) particles on the surface of composite 10-35 was not noticed.

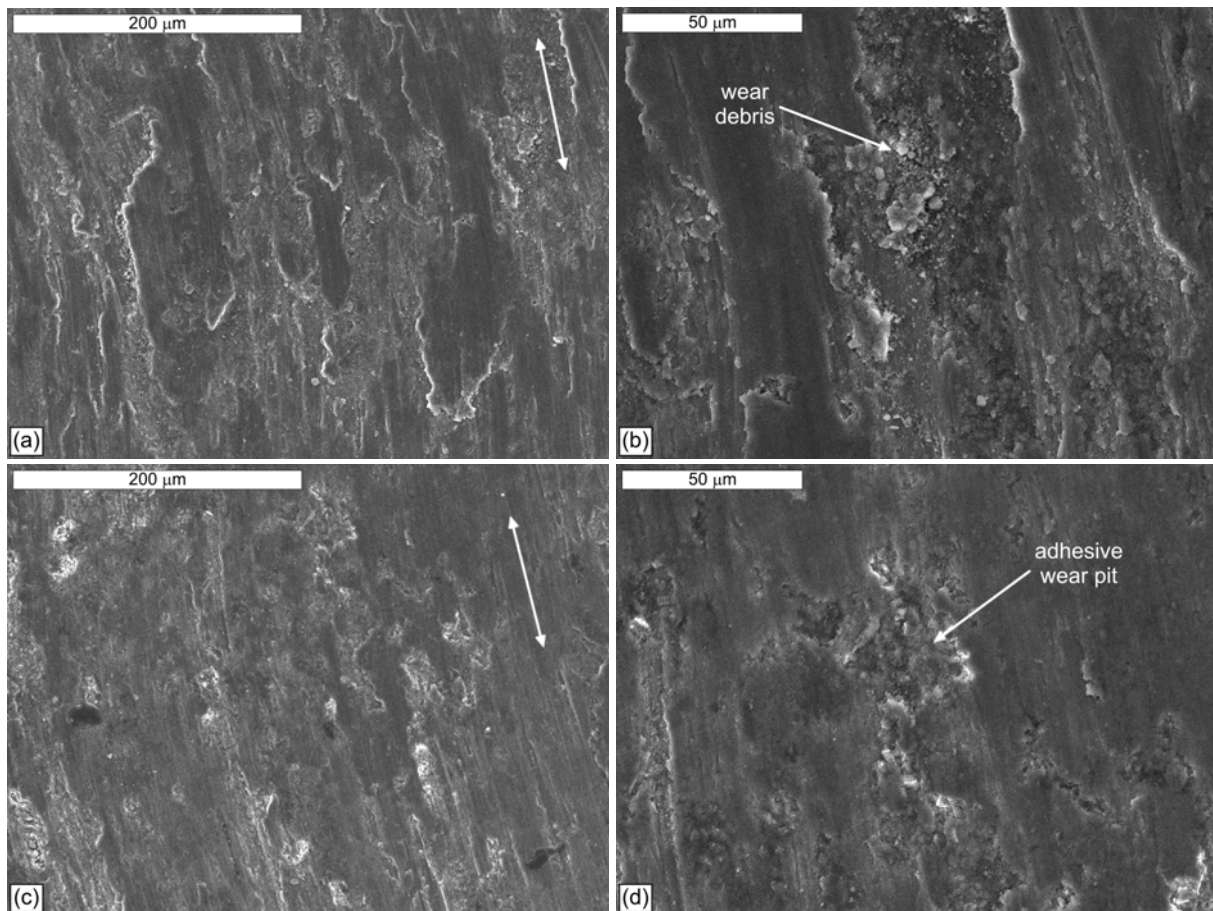


**Figure 8.** SEM micrographs of test samples worn surfaces: (a) and (b) A356 matrix alloy and (c) and (d) composite 10-35 (sliding directions is denoted with double arrows).

For the composites 10-39 and 10-39-1 dominant type of wear was also adhesive wear. Distinction of those two composites worn surfaces appearance from the composite 10-35 is presence of the protruded reinforcement particles (SiC particles in this case). Although the hardness of the composite with SiC particles was lower than the hardness of the composites with  $\text{Al}_2\text{O}_3$  particles the wear rates of those composite was also lower. This is due to the fact that the SiC reinforcements were protruded to the surface and thus protect the matrix alloy from further wear. Presence of those particles was more obvious for the composite 10-39-1 than for the composite 10-39 (Figures 9c and d) which is in correlation with their wear rates. Surface of the counter body was observed with OM and presence of transferred material was

noticed. This transfer was the largest for the contact with A356 matrix alloy (Figure 10).

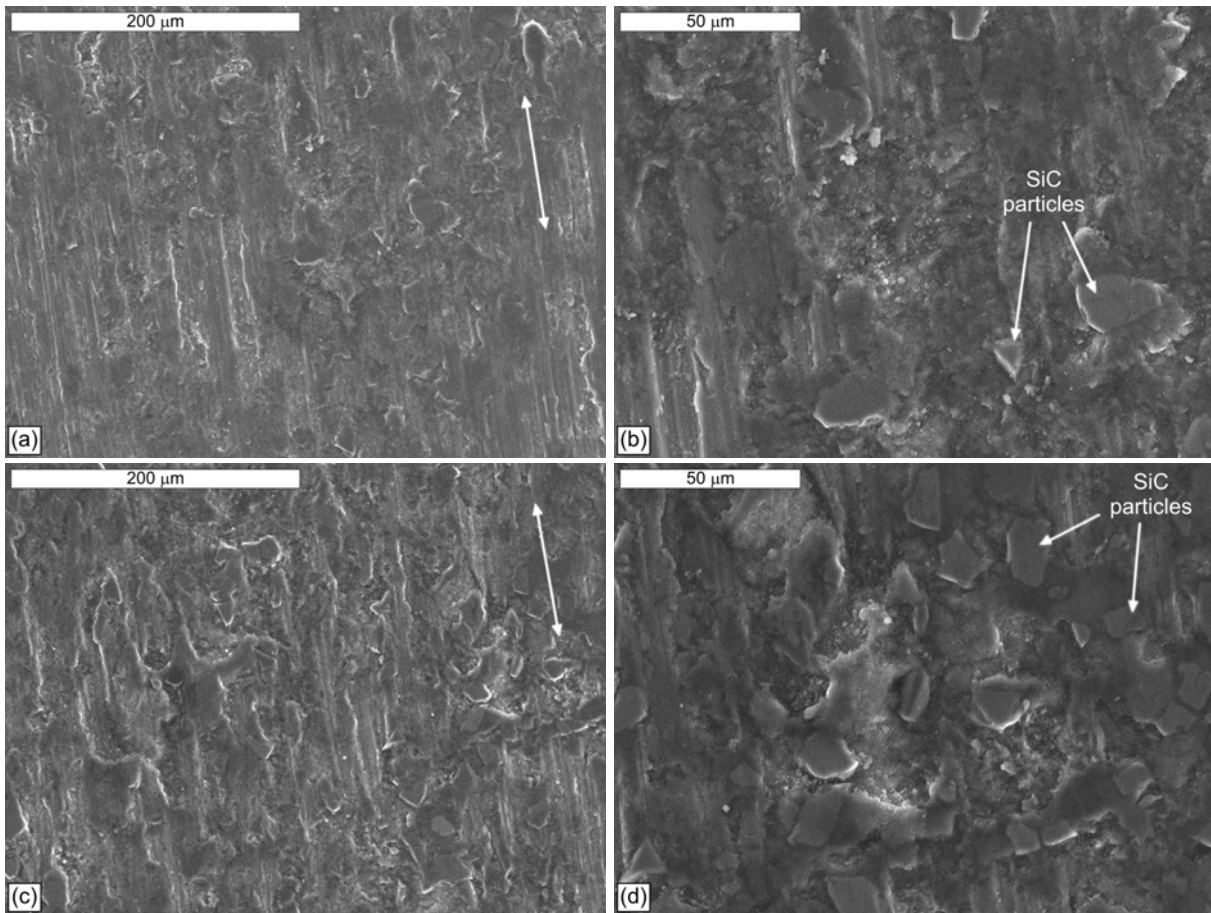


**Figure 9.** SEM micrographs of test samples worn surfaces: (a) and (b) composite 10-39 and (c) and (d) composite 10-39-1 (sliding directions is denoted with double arrows).

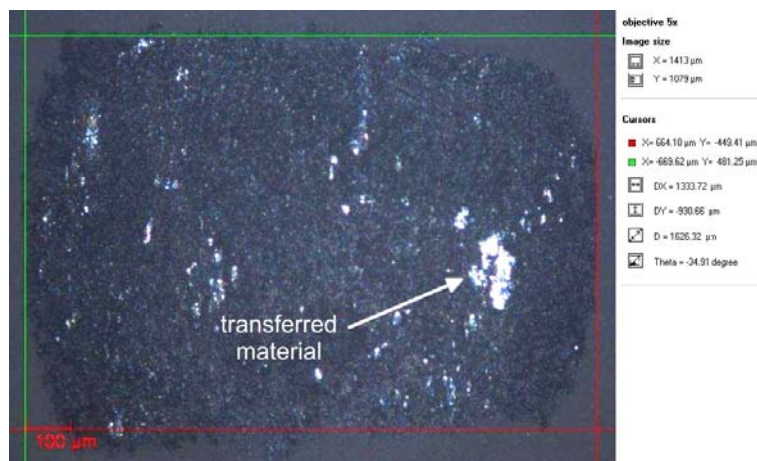


**Figure 10.** OM micrograph of the counter body worn surface (a counter body in contact with A356 matrix alloy).

Morphology and size of wear debris collected during the tests are shown in Figure 11. Debris generated by the wear of the materials in contact (counter body and corresponding sample) originate mostly from the test samples material. This is confirmed with the EDS analysis (Figure 12). Among the wear debris of A356 matrix

alloy (Figure 11a) and composite 10-35 (Figure 11b) prevail mainly sharp edge, plate-like particles, which is typical for adhesive wear.<sup>(14,15)</sup> On the surface of these plate-like particles presence of material plastic flow could be noticed. Size of the particles varied and in some cases individual particles, larger than 50  $\mu\text{m}$  in diameter, may be seen. This indicates existence of severe wear.<sup>(16)</sup> SEM microphotographs of composites 10-39 and 10-39-1 (Figures 11c and d) indicate that particles in the wear debris were also mainly plate-like with sharp edges, but the maximum sizes of those particles were smaller (app. 20  $\mu\text{m}$  in diameter) comparing with the debris of the other two material. The size of the particles in the wear debris is confirmed with the EDS analysis results (Table 3). In Table 3 only the main elements in wt. % are shown. As it is well known the smaller and finer particles oxidise easier, and for the composites 10-39 and 10-39-1 (smaller particles) the oxygen content was significantly higher than for the A356 matrix alloy and composite 10-35.

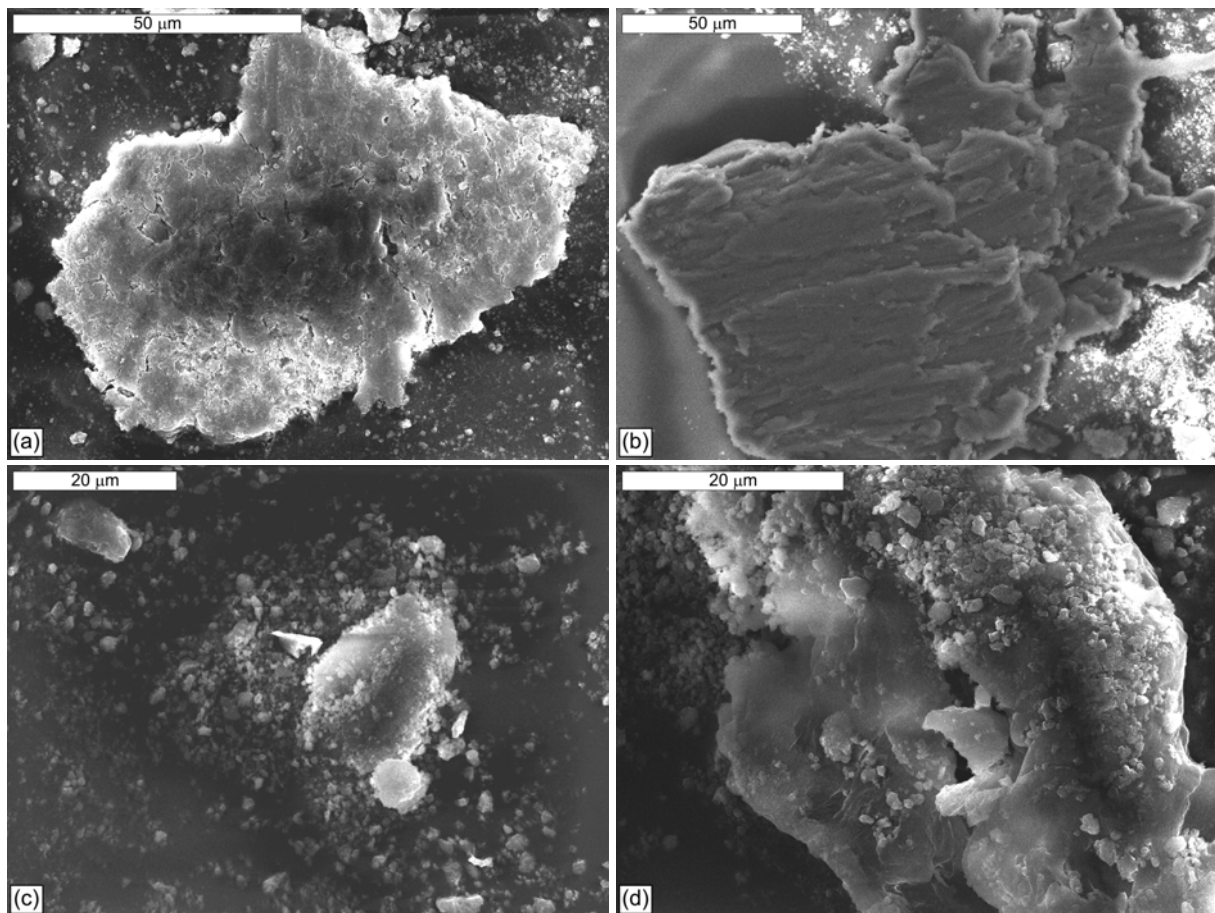


**Figure 11.** SEM microphotographs of the wear debris generated in contact of counter body with: (a) A356 matrix alloy, (b) composite 10-35, (c) composite 10-39 and (d) composite 10-39-1.

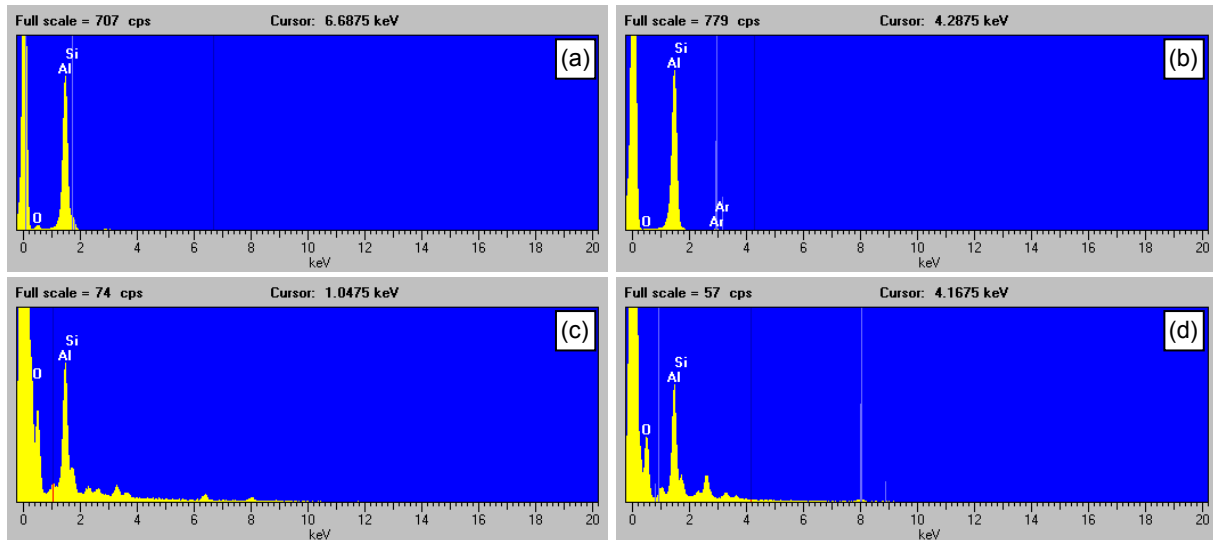


**Figure 12.** EDS analysis of the particles in wear debris (only main elements): (a) A356 matrix alloy, (b) composite 10-35, (c) composite 10-39 and (d) composite 10-39-1.

**Table 3.** EDS analysis results of the particles in wear debris (only main elements)

Material	Element, wt. %		
	O	Al	Si
A356 matrix alloy	24.95	62.59	12.47
Composite 10-35	13.82	80.80	5.39
Composite 10-39	68.72	24.33	6.95
Composite 10-39-1	69.04	24.29	6.67

## 4 CONCLUSIONS

The composite materials with better tribological properties in relation to matrix alloy can be obtained by compocasting process. All composite materials showed better tribological properties regardless their hardness values.

Wear resistance of the composites reinforced with SiC particles was higher and coefficient of friction was lower compared to the composite reinforced with Al<sub>2</sub>O<sub>3</sub> particles due to the higher hardness of the SiC particles, and due to the fact that the SiC reinforcements were protruded to the surface and thus protect the matrix alloy from further wear.

Addition of graphite particles (1 wt. %) to the composite with SiC particles further reduced the wear rate and the coefficient of friction but this influence should be considered only as a trend of behaviour since for each application there exists a range of optimal value of graphite particle content to produce material with good tribological properties.

## Acknowledgements

This work has been performed within the projects TR-14005 and TR-19205. Those projects are supported by the Republic of Serbia, Ministry of Science and Technological Development, which financial help is gratefully acknowledged.

## REFERENCES

- 1 SURAPPA, M.K. Aluminium matrix composites: challenges and opportunities. **Sādhanā**, v. 28, n. 1-2, p. 319-334, february. 2003.
- 2 ROHATGI, P. Cast aluminum-matrix composites for automotive applications. **JOM**, v. 42, n. 4, p. 10-15, april. 1991.
- 3 RIBES, H.; SUÉRY, M. Effect of particle oxidation on age hardening of Al-Si-Mg/SiC composites. **Scripta Metallurgica**, v. 23, n. 5, p. 705-709, may. 1989.
- 4 DAOUD, A.; REIF, W. Influence of Al<sub>2</sub>O<sub>3</sub> particulate on the aging response of A356 Al-based composites. **Journal of Materials Processing Technology**, v. 123, n. 2, p. 313-318, april. 2002.
- 5 MARINKOVIĆ, A.; VENCL, A. Influence of the solid lubricant particles reinforcement on composites tribological properties. In: 11<sup>th</sup> INTERNATIONAL CONFERENCE ON TRIBOLOGY – SERBIATRIB '09, 13-15.05.2009, Belgrade. p. 78-83.
- 6 LIU, Y.; ROHATGI, P.K.; RAY, S. Tribological characteristics of aluminum-50 vol pct graphite composite. **Metallurgical and Materials Transactions A**, v. 24, n. 1, p. 151-159, december. 1993.
- 7 ROHATGI, P.K.; LIU, Y.; RAY, S. Friction and wear of metal-matrix composites. In: BLAU, P.J. (Ed.). **ASM Handbook Vol. 18: friction, lubrication, and wear technology**. Metals Park: ASM International, 1992, p. 801–811.
- 8 BASAVARAJAPPA, S.; CHANDRAMOHAN, G.; MUKUND, K.; ASHWIN, M.; PRABU, M. Dry sliding wear behavior of Al 2219/SiCp-Gr hybrid metal matrix composites. **Journal of Materials Engineering and Performance**, v. 15, n. 6, p. 668-674, december. 2006.
- 9 YANG, J.B.; LIN, C.B.; WANG, T.C.; CHU, H.Y. The tribological characteristics of A356.2Al alloy/Gr(p) composites. **Wear**, v. 257, n. 9-10, p. 941-952, november. 2004.
- 10 VENCL, A.; BOBIC, I.; AROSTEGUI, S.; BOBIC, B.; MARINKOVIĆ, A.; BABIĆ, M. Structural, mechanical and tribological properties of A356 aluminium alloy reinforced with Al<sub>2</sub>O<sub>3</sub>, SiC and SiC + graphite particles. **Journal of Alloys and Compounds**, v. 506, n. 2, p. 631-639, september. 2010.
- 11 VENCL, A.; BOBIC, I.; JOVANOVIĆ, M.T.; BABIĆ, M.; MITROVIĆ, S. Microstructural and tribological properties of A356 Al-Si alloy reinforced with Al<sub>2</sub>O<sub>3</sub> particles. **Tribology Letters**, v. 32, n. 3, p. 159-170, december. 2008.
- 12 RANDALL, N. (Ed.). Overview of mechanical testing standards, In: **Applications Bulletin**: no. 18. Peseux : CSM Instruments, 2002, p.1-4.
- 13 FRANCO JR., A.R.; PINTAÚDE, G.; SINATORA, A.; PINEDO, C.E.; TSCHIPTSCHIN, A.P. The use of a Vickers indenter in depth sensing indentation for measuring elastic modulus and Vickers hardness. **Materials Research**, v. 7, n. 3, p. 483-491, july-september. 2004.
- 14 BOWEN, R.; SCOTT, D.; SEIFERT, W.; WESTCOTT, V.C. Ferrography. **Tribology International**, v. 9, n. 3, p. 109-115, june. 1976.
- 15 RAADNUI, S. Wear particle analysis – utilization of quantitative computer image analysis: A review. **Tribology International**, v. 38, n. 10, p. 871-878, october. 2005.
- 16 VAN DRIESCHE, M. **Ferrography**. Ghent: Texaco Technology Ghent, 2001.